CHAPTER 4

CONTROLLER DESIGN OF DFIG FOR WECS BY USING BIO-INSPIRED TECHNIQUES

4.1 Wind Turbine Systems for WECS

However, the wind velocity changes radically depending on the environmental circumstances along with the time of operation. Therefore, it has a huge margin of the speed difference. Such margins of speed alteration compose wound rotor induction machines appropriate for power generation through wind energy. Wind turbines can run either fixed speed (actually within a speed range about 1 %) or different speed [122]. For fixed speed wind turbines, induction generator is instantly coupled to the grid. Since the speed is nearly fixed to the grid frequency, and not controllable, it is not possible to store the instability of the wind in the form of revolving free energy. Hence, for a fixed-speed system, the turbulence of the wind will result in power fluctuations, which influence the power quality of the grid. The power electronic apparatus are used to control the variable-speed wind turbine and generator, which makes it probable to control the rotor speed.

4.1.1 Wind Turbine Aerodynamics model

The wind turbine aerodynamic model can be characterized by the well-known C_P (λ, β) curves [123], [132]. C_P is the power coefficient, which is a function of both tip-speed-ratio λ and the blade pitch angle β of WT. However tip speed ratio λ is defined as follows, i.e.

$$\lambda = \frac{w_t r}{V_w} \tag{1}$$

Now from above *r* is the blade length in m, ω_t is the wind turbine rotational velocity in rad/s, and V_w is the wind speed in m/s. Furthermore, numerator (ω_t r) represents the blade tip speed in m/s of WT. Whereas the C_P (λ, β) curves depend upon the blade design and also given by the wind turbine manufacturer. Here a scientific illustration of the C_P curves used for the 2MW wind turbine obtained by curve fitting in [123-132], [41,133] is given by following equations.

$$C_p(\lambda,\beta) = 0.22\left(\frac{116}{\lambda_i} - 0.4\beta - 5\right)e^{\frac{-12.5}{\lambda_i}} \tag{2}$$

$$\text{Here } \frac{1}{\lambda_i} = \frac{1}{\lambda + 0.08\beta} - \frac{0.035}{\beta^3 + 1} \tag{3}$$

For the given power coefficient C_P, the mechanical power that the wind turbine extracts from the wind is calculated by as follows

$$\text{Pm} = \frac{1}{2}\rho A v_w^3 \; C_P(\lambda, \beta) \tag{4}$$

Where ρ is the air density in kg/m^3, A = πR^2 is the area in m^{2}swept by the rotor blades. The turbine power characteristics at pitch angle zero are described in [41], [133].

WT based terms and definitions: The name and descriptions related to WT [22] are as follows.

Kinetic energy of air masses per unit time: Power contained in the wind as kinetic energy of air masses per unit time: $P_0 = \frac{1}{2} \times$ (Air mass per unit time) × (Wind Velocity)^3

$$P_0 = \frac{1}{2}\rho A \, (V_w)^3$$

Tip Speed Ratio (TSR): The ratio of the wind flowing from the tip of the blade to the wind velocity is known as Tip speed ratio (λ) as;

$$\lambda = \frac{\omega_t r}{v_\omega}$$

Now from above *r* is the blade length in m, ω_t is the wind turbine rotational velocity in rad/s, and v_ω is the wind speed in m/s. Furthermore, the numerator (ω_t r) represents the blade tip speed in m/s of WT.

Power coefficients:-The ratio of power output of the machine to the power contained in the wind is called as power coefficient. Cp denotes it.

$$C_p(\lambda,\beta) = 0.22\left(\frac{116}{\lambda_i} - 0.4\beta - 5\right)e^{\frac{-12.5}{\lambda_i}}$$

Where; $\frac{1}{\lambda_i} = \frac{1}{\lambda + 0.08\beta} - \frac{0.035}{\beta^3 + 1}$

Pitch Angle (β):-It is the angle between the chord of aerofoil section and the plane of revolution.

Mechanical power (Pm):- For the given C_P, the mechanical power that the wind turbine extracts from the wind is calculated by as follows;

$$\text{Pm} = \frac{1}{2}\rho A v_w^3 \; C_P(\lambda, \beta)$$

Where ρ is the air density in kg/m^3, A = πR^2 is the area in m^{2}swept by the rotor blades.

4.1.2 A Background on DFIG based wind turbine Components for WECS

Major components of DFIG based WTs are explained in [134]. Figure (4.1) shows the typical DFIG along with its parts.

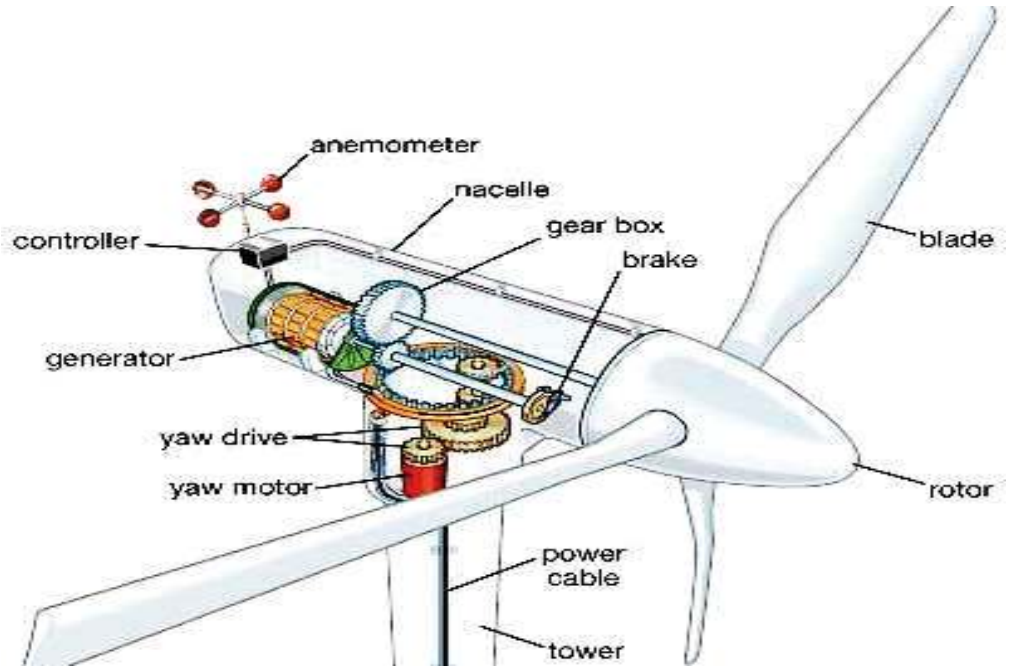

Figure 4.1: DFIG based Wind Turbine system

Rotor: it is composed of blades and a hub. Blades absorb the wind energy and transmit it to the hub. The receiving power of turbine is directly related to squared length of blades as pointed in.

Pitch motor: wind turbines equipped with pitch control, the blades turn to the wind direction according to Maximum Power Tracking (MPT).

Mechanical brakes: The connection shaft between gearbox and generator is equipped with mechanical brake systems which are disc type brakes.

Gearbox: Most DFIG units use a gearbox. The purpose of the gearbox is connected to the low-speed axis at one end and to electricity generator at the other end, to increase the low rate of rotor turn appropriately.

Generator: Generators used in DFIG based wind turbines are of induction type. The 3-phase stator winding is connected to the grid through a step up transformer. Rotor has a 3-phase

winding which is fed by a slip ring from the rotor side converter. Rotor current is controlled by this rotor side converter which consequently controls active and reactive powers.

Anemometer: An anemometer is a device that measures wind speed as well as wind pressure.

Controllers: it has several microprocessors and microcontrollers for controlling and coordination of different parts of the DFIG.

Sensors: In each DFIG based WTs, sensors of different types are used to provide information such as wind direction, wind intensity, rotor speed, voltage, current, output power, heat indicators, gearbox oil, hydraulic system gauges and so on.

Nacelle: Nacelle holds main components of a wind turbine like gearbox, generator, shaft and other parts. The rotor is located at Nacelle head while sensors for wind speed are placed at end.

Yaw motor: This system employs two or more electric motors for rotating the nacelle in the wind direction. That's controlled from a central control room which recognizes the wind direction based on data from sensors and sends the necessary commands to motors.

Tower: Nacelle with blades is mounted on a tower. In general, the higher tower is better because wind speed increases with height from the ground. In a 2MW generation, DFIG based wind turbine has the tower height is about 50 to 80 meter.

Converters: A DFIG based WT uses two converters grid and rotor side. DFIG can operate both in super and sub-synchronous modes requiring the converter to work bi-directionally.

4.2 Impression and operational theory of DFIG

DFIG is one of the most frequently used generators in the wind energy industries [35].Currently, such generators are extensively accepted as one of the appropriate wind energy conversion systems, which is depicted in Figure (4. 2).

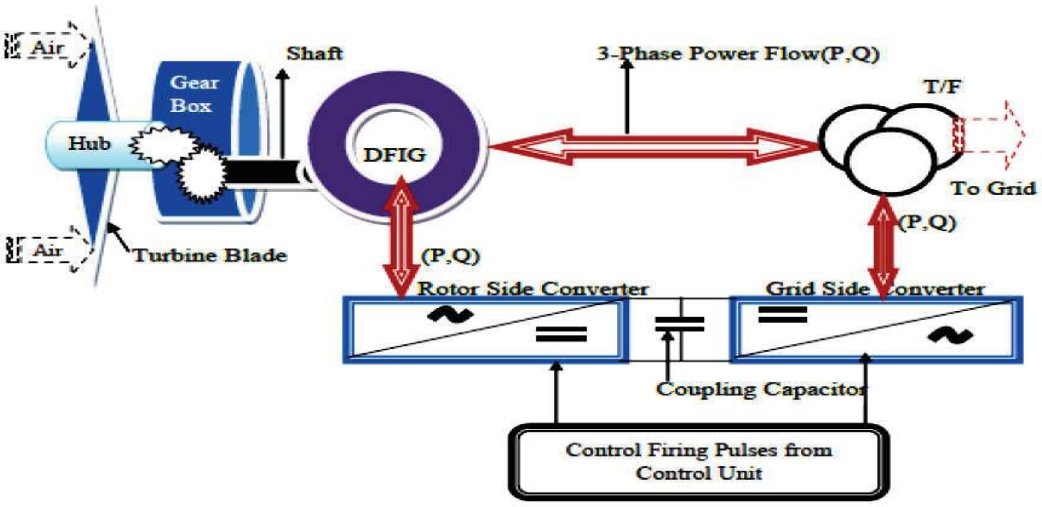

Figure 4.2: Typical installation diagram of DFIG for WT

DFIG is in nature a wound rotor induction generator, and the rotor circuit is usually controlled by electric power devices to allow variable speed operation. The detail descriptions about DFIG along with principle of operation as well as 6th order Transfer function of the DFIG system is presented in chapter 2. On the other hand the 6th order relations, in the form of the Transfer function of the reduced model to the DFIG system is presented in [46]. As follows;

$$G(S) = \frac{0.000324s6 - 1.75s5 - 2366s4 + 7.9e6s3 + 7.5e9s2 + 5e12s + 2.18e14}{s6 + 2340s5 + 8.67e6s4 + 4.79e9s3 + 2.7e12s2 + 1.27e14s + 9.6e14} \quad (5)$$

4.3 Bacterial Foraging Optimization

The impression and brief description for bacterial foraging optimization with algorithmic features are described in [135-139].

Based on the research of foraging behavior of E.colli bacteria Kevin M.Passino and Liu exploited a variety of bacterial foraging and swarming behavior, discussing how to connect social foraging process with distributed non-gradient optimization. In the bacterial foraging optimization process four mobile behaviors are mimicked:

(1) Chemotaxis:

A chemotactic step can be defined as a tumble followed by a tumble or a tumble followed by a run lifetime. To represent a tumble a unit length random direction, X (j), is generated; this will be used to define the direction of movement after a tumble.

In particular $X^i(j+1,k,l) = X^i(j,k,l) + C(i)*X(j)$,

Where $X^i(j,k,l)$ represents the i^{th} bacterium at j^{th} chemotactic, k^{th} reproductive and l^{th} elimination and dispersal step.C(i) is the size of the step taken in the random direction specified by a tumble(the run length unit).

(2) Swarming:

E.Colli cells can work cooperatively self-organize into highly structured colonies with high environmental adaptability using a complex communication mechanism. Overall, cells provide an attraction signal to each other, so they swarm together. The mathematical representation for swarming can be represented by

$$Jcc(\theta,P(j,k,l)) = J^i cc(\theta,\theta^i(j,k,l)) = \Sigma[\, D \text{ attract} * EXP(-W \text{ attract} * \Sigma(\theta m - \theta^i m)^2)]$$

$$+\Sigma\,[H \text{ repellant} * EXP\,(-W \text{ repellant} * \Sigma\,(\theta m - \theta^i m)^2)]$$

Where Jcc(θ, P(j,k,l)) is the cost function value to be added to the actual cost function, that is to be minimized to present a time-varying cost function. S is the total number of bacteria , P is the number of parameters to be optimized which are found in each bacterium and D attract, W attract,h repellant, W repellant are different coefficients that should be appropriately chosen.

(3) Reproduction:

The least healthier bacteria die and the other each healthier bacteria split into two new bacteria each placed in the same location.

(4) Elimination and Dispersal:

It is possible that in the local environment, the lives of a population of bacteria changes either gradually (e.g., via consumption of nutrients) or suddenly due to some other influence. Events can occur that all the bacteria in a region are killed, or a group is dispersed into a new part of the environment. They have the effect of possibly destroying the chemotactic progress, but they also have the effect of assisting the chemotactic process, since dispersal may place bacteria near good food sources. From a board perspective, elimination and dispersal are parts of the population level long distance mobile behavior. However, BFO algorithm procedure as flow chart along with pictorial representation of swim and tumble of a bacterium is shown in Figure (4.3&4.4) [139].

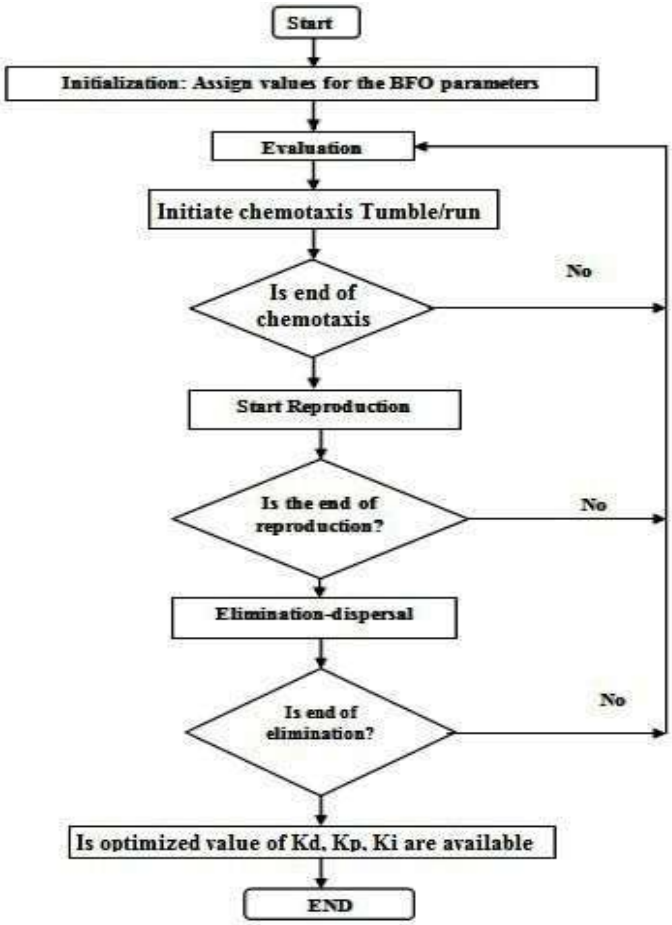

Figure 4.3: BFO algorithm process as flowchart

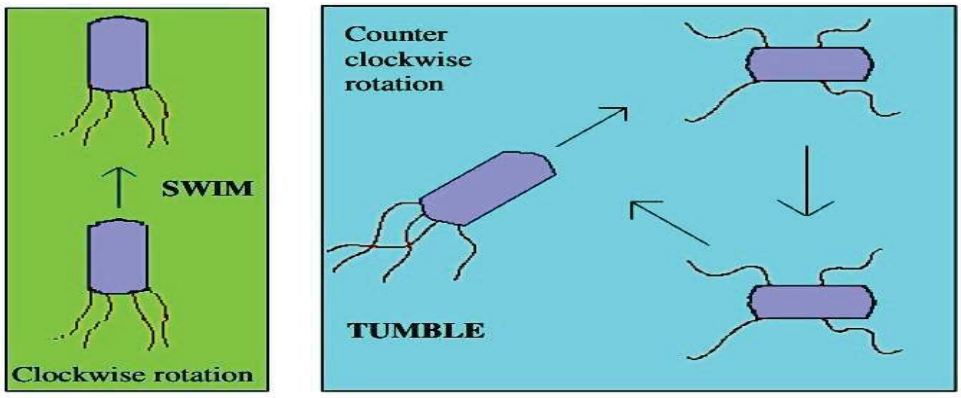

Figure 4.4: Pictorial representation of swim and tumble of a bacterium

4.3.1 Algorithm for Bacterial Foraging Optimization-Based Design

The searching procedures of the proposed BF-PID controller is as follows:-

Step 1)

Initialize parameters S , D , NS,NC , Nre Ned ,Ped , X ,C(i), D attract ,W attract, H repellant

And W repellant, where

S: Number of bacteria to be used for searching the entire region.

D: Number of parameters to be optimized.

NS: Swimming length after which tumbling of bacteria will be done in a chemotactic step.

Nre: Maximum number of reproductions to be undertaken.

Ned: Maximum number of elimination-dispersal events to be imposed over the bacteria.

Ped: Probability with which the elimination-dispersal will continue.

X: The location of each bacterium which is specified by random numbers on [0, 1]

C (i): This is chemotactic step size assumed constant for our design.

Step 2)

Elimination-Dispersal loop: l=l+1

Step 3)

Reproduction loop: k = k+1

Step 4)

Chemotaxis loop: j = j + 1

a) For i = 1,2,3,4.....S, take a chemotactic step for i as bacterium follows.

b)Compute J(i, j,k,l)

let J(i, j,k,l) = J(i, j,k,l) + JCC(i (j,k,l),P(j,k,l)) (i.e. add on the cell-to-cell attractant effect to the nutrient concentration).

c) Let J Last = J (i, j, k, l) to save this value since we may find a better cost via run.

d) Tumble: Generate a random number vector (i) € R_P with each element m (i),

m= 1, 2, 3 ...D, a random number on [-1, 1].

e)Move

Let i(j+1,k,l) = i (j,k,l) + C(i)* (i)/(sqrt(T (i)* (i))).

The results in a step size C (i) in the direction of the tumble for bacterium i.

f) To Compute J(i, j,k,l), and then let J(i, j,k,l) = J(i, j,k,l) + JCC((j,k,l),P(j,k,l))

g) Swim: note that we use an approximation since we decide swimming behavior of each cell as if the bacteria numbered {1,2,.....,i} have moved, and {i+1,i+2,i+3.....S} have not; this much is simpler to simulate than simultaneous decisions about swimming and tumbling by all the bacteria at the same time:

Let m = 0 (counter for swim length).

While m<NS (if NS have not climbed down too long)

Let m= m+1

If J (i, j, k, l) < JLast (if doing better), let

JLast = J (i, j+1, k, l) and let

$$X^{i}(j+1, k, l) = X^{i}(j, k, l) + C(i) * X(i) / (\text{sqrt}(X^{T}(i) * X(i)))$$

and use $X^{i}(j+1,k,l)$ to compute the new J(i,j+1,k,l) as we did in f).

.Else,

let m = NS, this is the end of the while statement.

h) Go to next bacterium (i+1) if 'i' is not equal to S (i.e., go to (b)) to process the next bacterium.

Step 5)

If j < NC go to Step 3 In this case, continue Chemotaxis, since the life of the bacteria is not over.

Step 6)

Reproduction:

a) For a given k and l, and for each i = 1,2,3,4.....S, let J^{i} Health = Σ J (i, j, k, l) be the health of the bacterium (a measure of how many nutrients it got over its lifetime and how successful it was at avoiding noxious substances). Sort bacteria on chemotactic parameters C (i), in order of increasing cost J Health (higher cost means lower health) of the bacterium.

b) The Sr bacteria with highest J Health value die, and the other Sr bacteria with the best values split, and the copies that are made and placed at the same location as their parent.

Step 7)

If k<Nre, go to step 2. In this case, we have not reached the number of specified reproduction steps, so we start the next generation in the next chemotactic step.

Step 8)

Elimination-Dispersal: For i = 1,2,3,4.....S, with probability Ped, eliminate and disperse each bacterium (this keeps the number of bacteria in the swarming population constant). To do this, if we eliminate a bacterium, just disperse one into a random location within the optimization domain.

Step 9)

If l < Ned, then go to the step 1, otherwise end.

4.3.2 BFO based controller gain

The BFO based controller gains for the 6th order Transfer function reduced the model to the DFIG system [46], at the fitness function (function F = Fitness (K_D K_P K_I)) by several iterations which are given in Table (4.1).

Table 4.1: Gains of the BFO-based controller

Parameters	K_P	K_I	K_D
Gains	0.1417	0.1472	0.1005

4.4 Particle Swarm Optimization (PSO)

An overview and brief description for particle swarm optimization along with algorithm features as well as conception of fitness function to the controller design and Gains of the PSO-based controller has been described in chapter 3.

4.5 Simulation along with results

4.5.1 Simulink response of DFIG system

The details description of DFIG Average Model (MATLAB) for 9 MW wind farm with the DFIG driven by a variable speed wind turbine has been described in previous chapter 3. The response of the DFIG based wind turbine with BFO based controller gain and PSO based PID controller regarding voltage along with current at the terminals, active power generated; reactive power requirements and DC capacitor voltage, as well as generator speed, are shown in Figure (4.5 to 4.16) respectively.

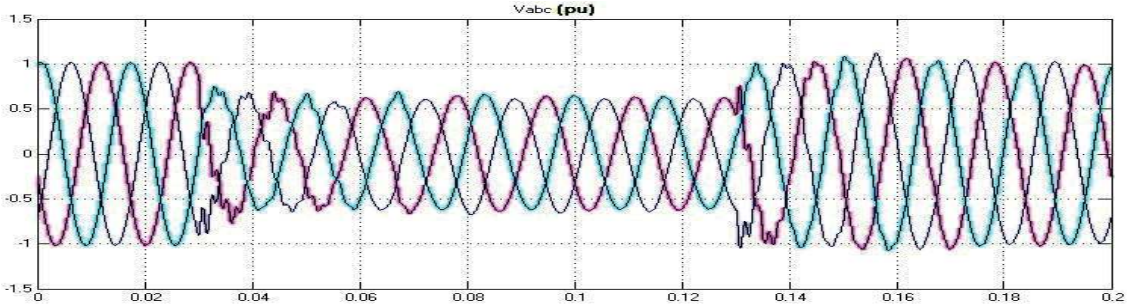

Figure 4.5: DFIG terminals Voltages in Pu (PSO based controller)

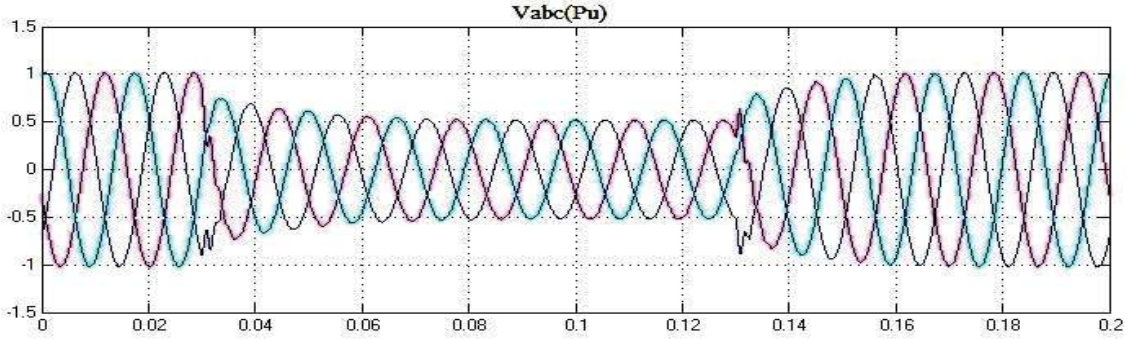

Figure 4.6: Voltages at the DFIG terminals in Pu (BFO-based controller)

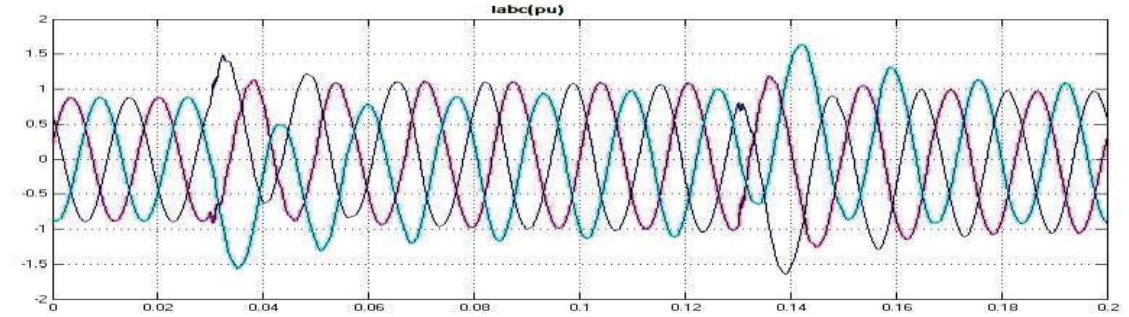

Figure 4.7: DFIG terminals Currents in Pu (PSO- based controller)

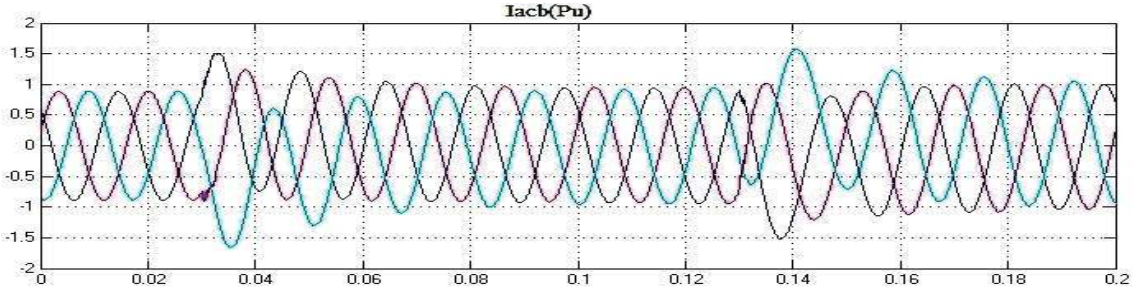

Figure 4.8: Currents at the DFIG terminals in Pu (BFO-based controller)

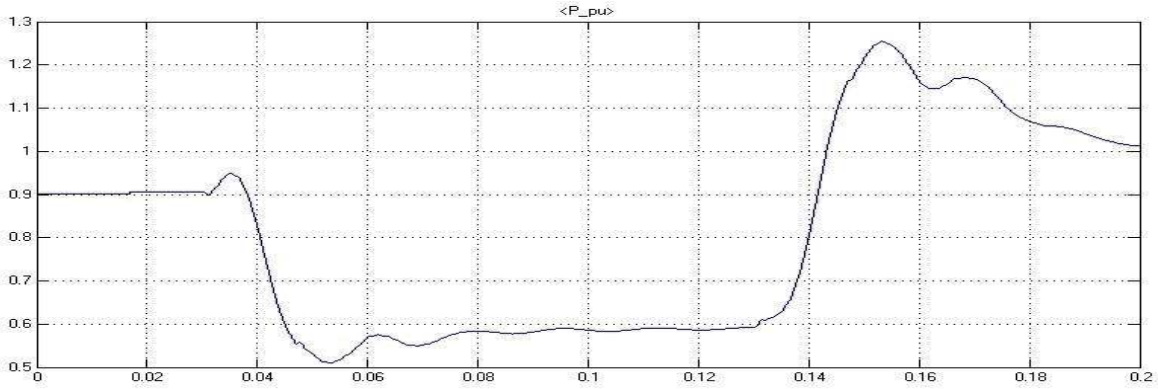

Figure 4.9: DFIG's Active power delivered in Pu (PSO based controller)

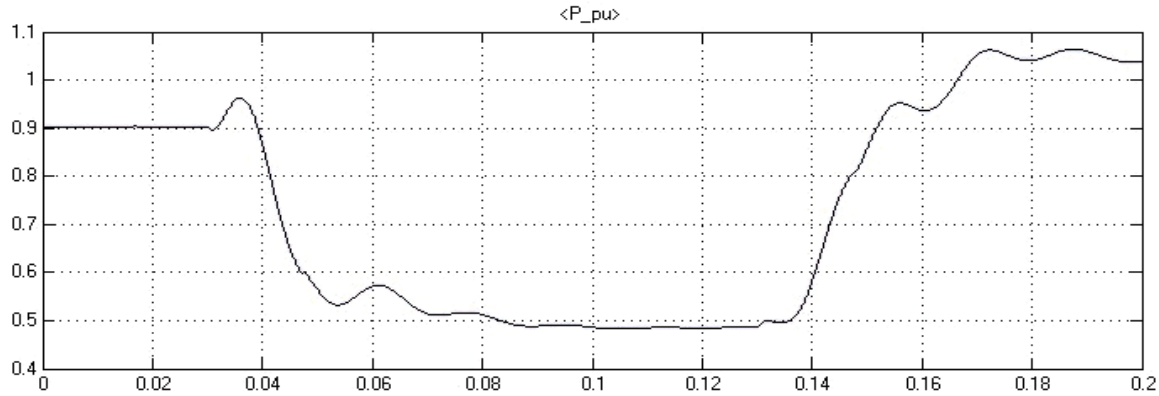

Figure 4.10: Active power given of the DFIG in Pu (BFO-based controller)

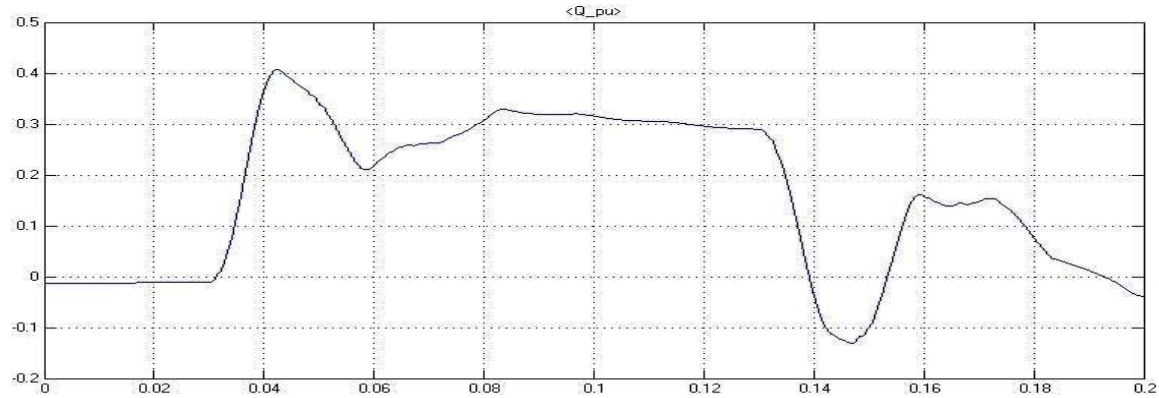

Figure 4.11: DFIG's Reactive power requirement in Pu (PSO based controller)

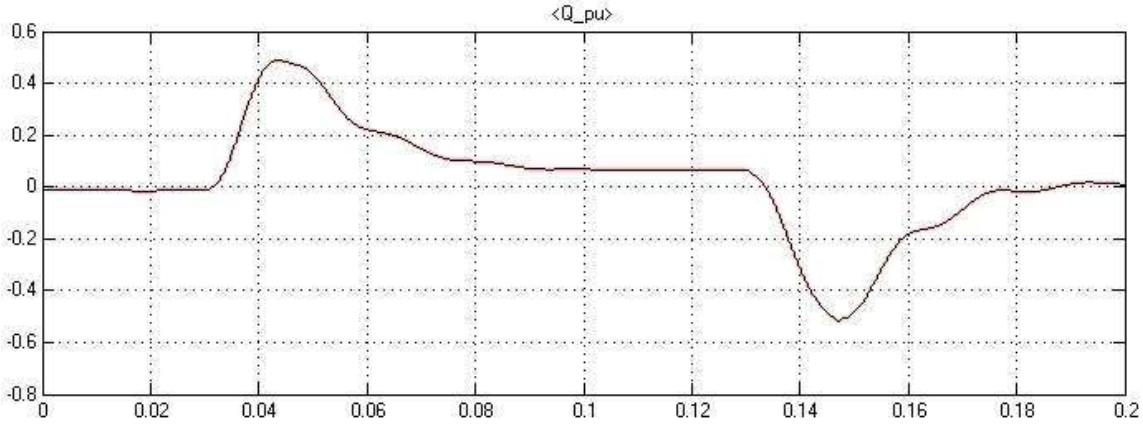

Figure 4.12: Reactive power requirement of the DFIG in Pu (BFO-based controller)

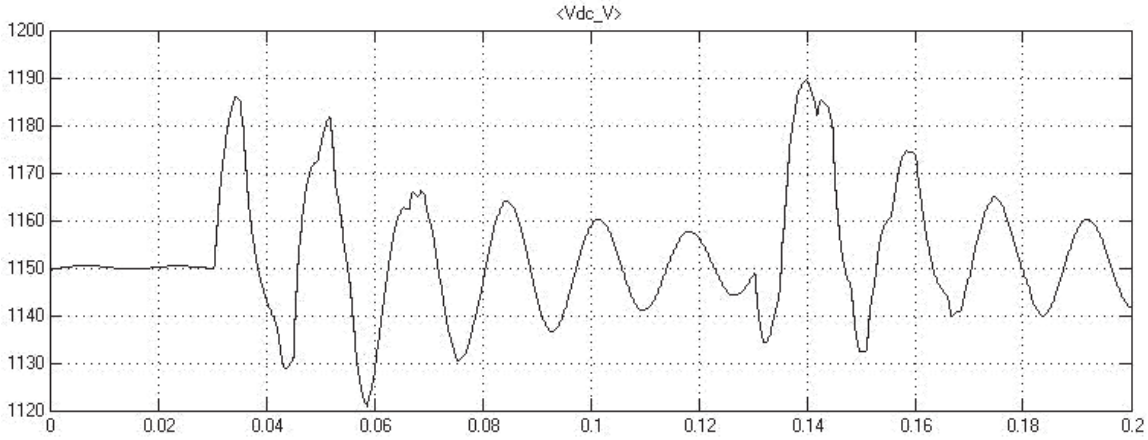

Figure 4.13: DC link voltage at the ordinary linkage capacitor (PSO based controller)

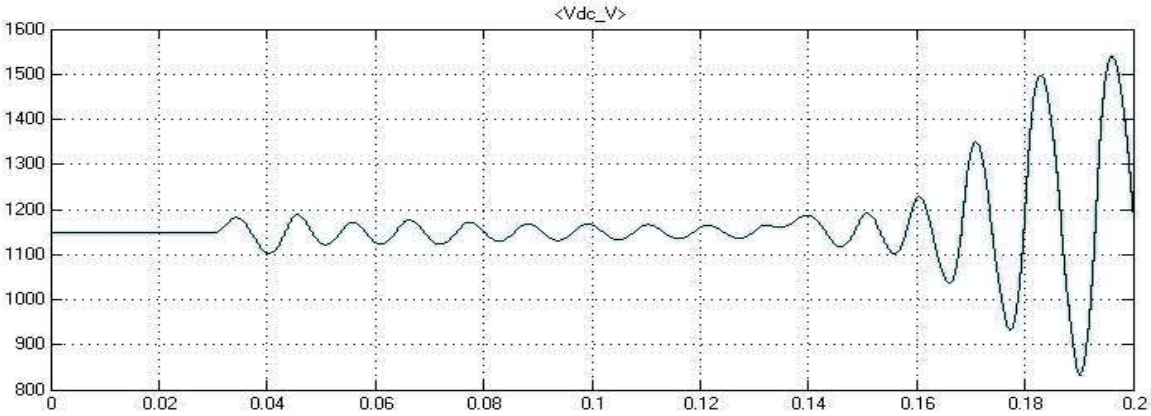

Figure 4.14: DC link voltage at the general coupling capacitor (BFO-based controller)

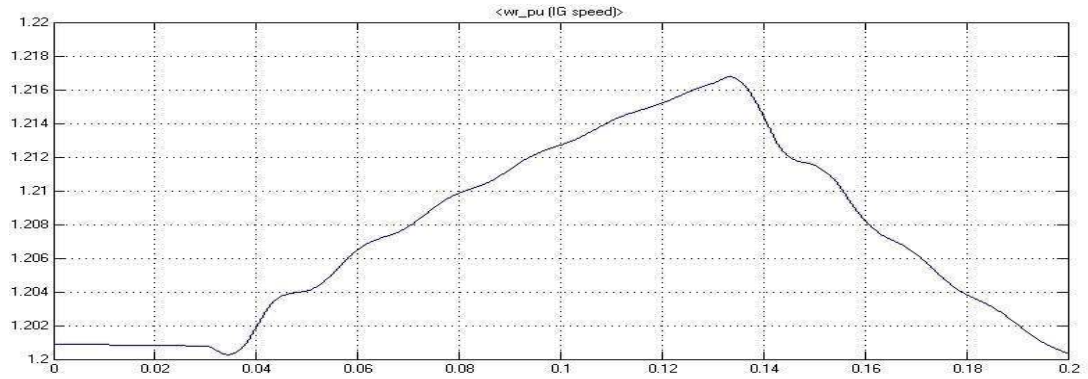

Figure 4.15: DFIG supported wind turbine speed in Pu (PSO based controller)

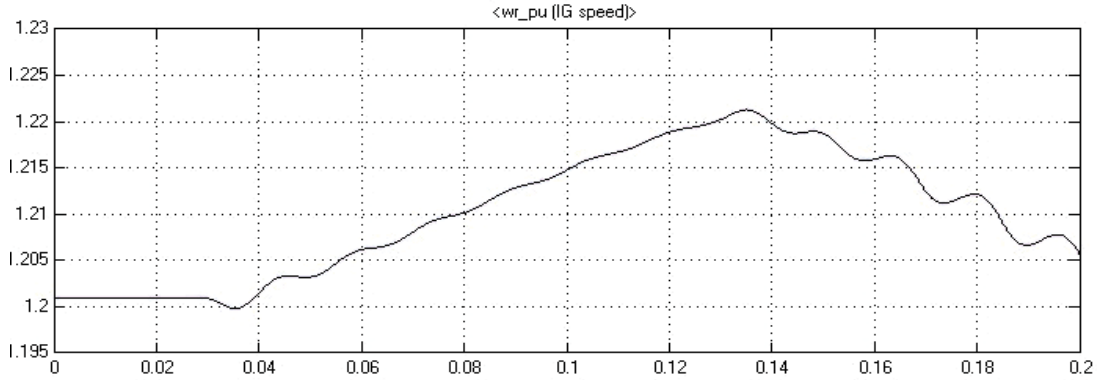

Figure 4.16: DFIG supported wind turbine speed in Pu (BFO-based controller)

Here Figure(4.5-4.16) concluded that the response of the DFIG system regarding terminal voltage, current, active-reactive power and DC-Link voltage along with generator speed slightly improved with PSO based controller instead of a BFO based controller.

4.5.2. BFO based Control Response by PID Controller

The reaction of the BFO based PID controller intended in [46, 134], and system in revise is as publicized in Figure (4.17). Here open loop system even though stable with steady state error100%, and the system has zero undershot in the response of open loop system. However, the step response of BFO based PID-controller in [46, 134] is shown in Figure (4.17).

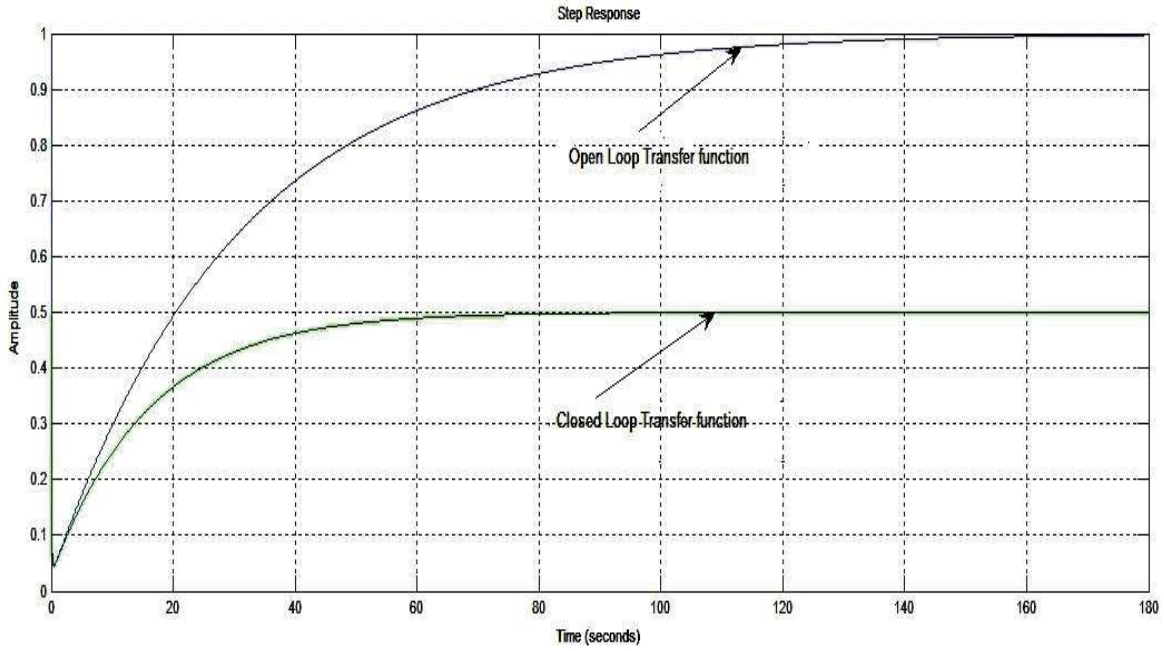

Figure 4.17: Step response of BFO based PID controller

The step response of Figure (4.17) has the following observations as shown in Table (4.2)

Table 4.2: step response observations of Figure (4.17)

Rise Time	Settling Time	Settling Min	Settling Max	Over Shoot	Under Shoot	Peak	Peak Time
0.00 sec	62.3541 sec	0.0438 sec	0.4992 sec	0.0 %	0.0 %	0.5000	0.0 sec

4.5.3. Response of PID Controller Using PSO Method

By using PID controller parameters which are designed in the previous chapter 3 Table (3.1). The step response of the system in revised for BFO based PID controller has been investigated, and step response of the system is exposed as in Figure (3.17). It is observable by a comparison result of BFO based PID control [46] along with one describe in this work which shows that; PSO based PID controller has extended to sufficiently damped BFO based controller without compromising the speed of response to the control loop. Now the step response of open as well as close loop reduced order system [46] by PID controller with PSO technique is shown in Figure (3.17).

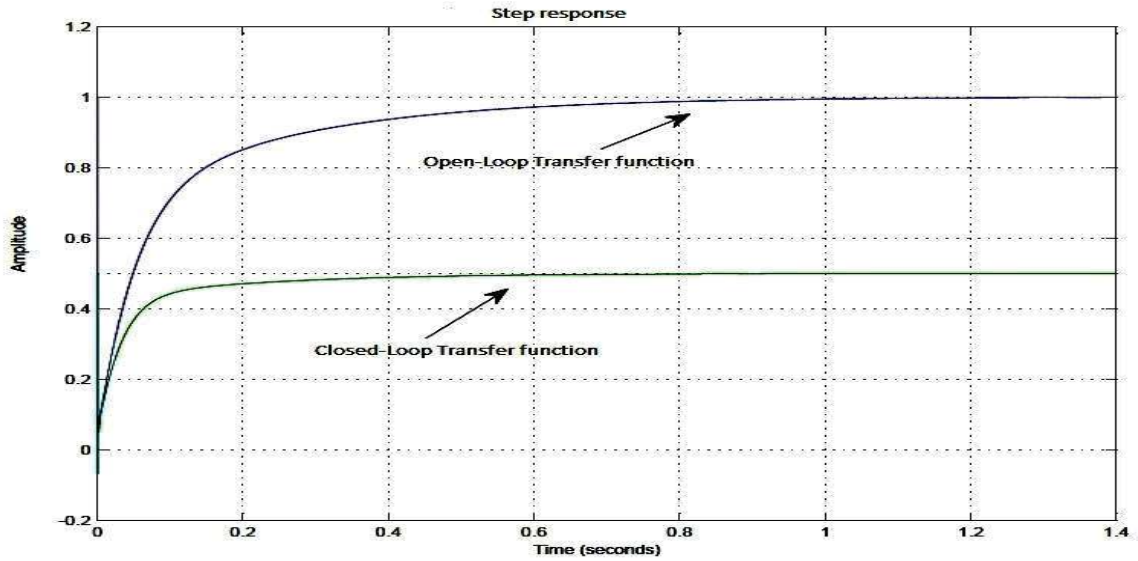

Figure 3.17: Step response of the PSO-based PID controller

The step response of Figure (3.17) has the following observations as shown in Table (3.2)

Table 3.2: step response observations of Figure (3.17)

Rise Time	Settling Time	Settling Min	Settling Max	Over Shoot	Under Shoot	Peak	Peak Time
0 sec	0.4061 sec	-0.0694 sec	0.4996 sec	0 %	13.8754%	0.500	0 sec

4.5.4 Comparison between BFO based and PID-controller using PSO method

Comparison of Rise time, Settling time, Peak time, Overshoot and Peak are given in Table (4.3). The performance parameters comparison to the controllers are presented in Table (4.3). which is concluded as:

(i) The designed PSO based PID controller can reduce the steady state error to zero as the existing one.

(ii) The rise time, peak time and overshoot have been reduced to zero, and the response is no more underdamped.

(iii) The speed response is much better than that of the current controller. Hence intended controller in this chapter assists to eliminate reactive power variations in DFIG system.

Table 4.3: Comparison of Rise time, Settling time, Peak time and Overshoot as well as Peak between BFO and PSO based PID controller

Controllers	Rise Time	Settling time	Peak Time	Overshoot	Peak
BFO based PID	0	62.3541	0	0	0.5000
PSO based PID	0	0.4061	0	0	0.5000

The publication from this part of the thesis work is as follows;

- **Om Prakash Bharti, R. K. Saket, S.K. Nagar, "**Controller Design of DFIG Based Wind Turbine by Using Evolutionary Soft Computational Techniques**", Engineering, Technology & Applied Science Research, Vol. 7, No. 3, 2017, 1732-1736. Indexed in ESCI (Thomson Reuters/Web of Science).**

4.6 Conclusion

The BFO based PID controller improves system responses, as compared with the open loop system along with rise time,peak time and overshoot to zero. Whereas PSO based designed controller not only enhances the system response but also reduces the percentage overshoot equal to zero. The obtained results show that the system using PSO based controller settles down in less time than the BFO based PID controller scheme. The comparison between PSO based controller and the BFO based PID controller are described precisely. It is concluded that the settling time is reduced next to 62 percent approximately and the percentage overshoot, rise time, peak time, etc. are reduced to zero using proposed method. Finally, it is concluded that the PSO control technique provides another option to design a reliable and adequate controller for implementation in the DFIG based wind energy conversion systems.

As the combined study among the various optimization Technique based controller design for DFIG based Wind Turbine system has not been carried out yet for the performance enhancements. Therefore, in chapter 5, an attempt is made to analyze how DFIG based WT system is influenced, when various types of controllers are designed by using GA, DE and FFA optimization techniques are taken into account.